Evidence-based Conservation

Lessons from the Lower Mekong

Edited by Terry C.H. Sunderland
Jeffrey Sayer
Minh-Ha Hoang

ISBN 978-1-84971-394-8 (hbk)
ISBN 978-0-203-12846-6 (ebk)

Sunderland TCH, Sayer J and Hoang M-H (ed). 2013. *Evidence-based conservation: lessons from the lower Mekong*. Bogor, Indonesia: CIFOR.

Cover photo © Terry C.H. Sunderland

First published 2013 by Routledge
2 Park Square, Milton Park, Abingdon, Oxon OX14 4RN
Simultaneously published in the USA and Canada by Routledge
711 Third Avenue, New York, NY 10017
Routledge is an imprint of the Taylor & Francis Group, an informa business

CIFOR
Jl. CIFOR, Situ Gede
Bogor Barat 16115
Indonesia

T +62 (251) 8622-622
F +62 (251) 8622-100
E cifor@cgiar.org

cifor.org

20 Forest degradation in the Lower Mekong and an assessment of protected area effectiveness *c*.1990–*c*.2009

A satellite perspective

Dan Slayback and Terry C.H. Sunderland

In response to the current biodiversity crisis, there has been an exponential increase in the number of protected areas (PAs) and, correspondingly, the area under protection in recent years (Chape *et al*., 2005). The global network of protected areas now covers 11.5 per cent of the world's surface area (Rodrigues *et al*., 2004) with 8.4 per cent of this total protected area falling within categories I–IV of the IUCN's classification (Schmitt *et al*., 2009); the highest levels of protection. Although it is considered that the social costs of protected areas are considerable, the establishment of protected areas remains the primary means of achieving biodiversity conservation (Hutton *et al*., 2005). But in terms of direct biodiversity conservation outcomes, just how effective are protected areas and how do we measure "effectiveness", in terms of change in forest cover over time?

As remote sensing techniques have become increasingly available and cost-effective, quantitative information derived from studies reporting land use/cover change have become more widely used as a tool to test this effectiveness. Although changes in forest cover alone are not sufficient to represent complex landscape-scale dynamics, particularly understanding drivers of deforestation and degradation (Porter-Bolland *et al*., 2011), it is possible to provide an indication of the effectiveness of differing land cover and management arrangements through land cover change assessments (Rayn and Sutherland, 2011).

To complement the site-specific studies presented in this book, we also wanted to look at forest cover change in the protected areas of the Lower Mekong in order to provide a regional context. In particular, we wanted to examine how forest cover has, or has not, been affected by the existence of the various protected areas. These PAs include a wide range of protection designations, ranging from national parks to nature reserves. One might expect that the establishment and effective management of a PA would lead to lower forest degradation within its boundaries. However, in some circumstances, the

opposite can occur: if the PA is not well enforced, it may be viewed as a common resource (Hardin, 1968), particularly if enforcement results in non-compliance with local regulations (Robbins *et al*., 2006). Alternatively, if the boundary is well enforced and respected, the immediately surrounding areas may suffer from disproportionate pressure because the resources within the PA are inaccessible (Rayn and Sutherland, 2011).

We examine forest degradation over two approximately decade-long time intervals (driven by available satellite data) – *c*.1990–*c*.2000, and *c*.2000–*c*.2009 – and for two geographic zones – within the protected areas proper, and within an adjacent buffer zone extending 10 km from each PA boundary. Note that these buffer zones have no legal status and are only defined for the purpose in this analysis of comparing change inside a PA with change in the immediate wider region. We consider forest degradation to include both outright deforestation (conversion of forest to a non-forest landcover, such as agriculture or pasture) and degradation proper, in which the resulting landcover may still have tree cover, but at a substantially reduced density. We include both processes because degradation is often more likely to occur than deforestation and may or may not precede deforestation. Some forests may be degraded for use in agroforestry systems and then essentially recover. Such activity may well not be captured if the study only examined deforestation. However, degradation is inherently more difficult to capture because the change in vegetation density is not likely to be as dramatic as occurs with deforestation.

Data

Satellite imagery provides the only practical way to quantify forest degradation in and around the fifteen protected areas (PAs) of interest in the Lower Mekong (Table 20.1), which are spread across a 1,300-km-long region from northern Laos to southern Vietnam (Figure 20.1), and cover a total of nearly 30,000 km^2.

Landsat imagery is well suited to detecting changes in vegetation cover and condition because it contains several spectral bands in the vegetation-sensitive infrared and has a large historical archive. For this study, Landsat Thematic Mapper (TM, onboard the Landsat 4 and 5 satellites) and Enhanced Thematic Mapper (ETM+, on Landsat 7) imagery was acquired from the US Geological Survey's EDC (Earth Resources Observation and Science (EROS) Data Center, http://eros.usgs.gov). This imagery is provided at 30-m spatial resolution, and contains six spectral bands covering the visible, near-infrared, and mid-infrared. Most of the imagery is available as a "L1T" (Level 1 Terrain-corrected) product, which includes orthorectification sufficient to allow precise overlap of images from different dates. However, for a few images, the orthorectification was insufficient to allow direct overlap. Those images required further preprocessing before analysis.

The Landsat 7 instrument suffered a hardware failure in mid-2003, when its scan-line corrector (SLC) failed, and this has impacted all imagery acquired after that date by introducing long east-west oriented gaps in the imagery. For

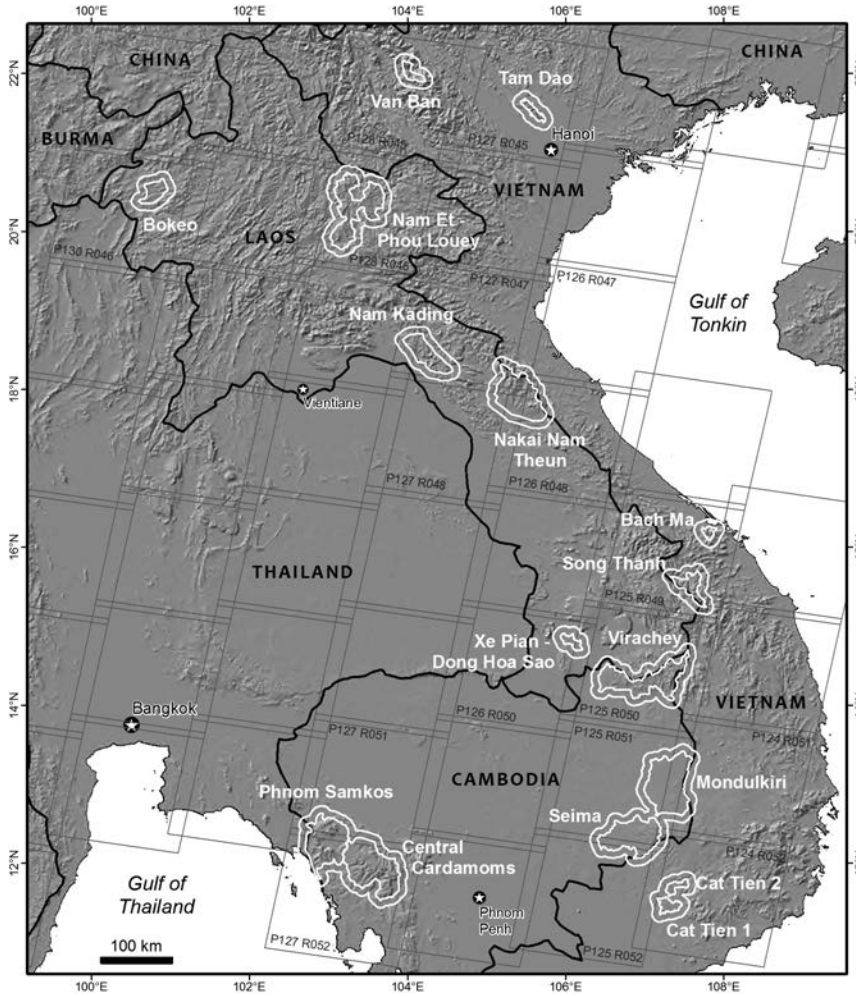

Figure 20.1 Regional overview showing the Lower Mekong protected areas and 10 km buffer zones outlined in white. Landsat image boundaries and scene numbers shown in grey

Source: Generated by Dan Slayback, NASA.

post-2003 dates, therefore, imagery from the Landsat 5 instrument was preferred when available, but due to other issues with Landsat 5 (which was launched in 1984 and has continued functioning for more than twenty years past its design lifetime), the number of images available from it is also limited.

Due to changes in data collection policies, and satellite downlink capacity, the available imagery in the archive varies substantially by date. From the early 1980s through 1999, when only Landsat 4 and 5 were in orbit, there is substantially less imagery available than since 1999, when Landsat 7 was launched.

Table 20.1 Protected areas analysed in this study, and corresponding areas

Country	*Site*	*Area (km^2)*
Cambodia	Central Cardamom Protected Forest	4,140
	Mondulkiri Protected Forest	4,080
	Phnom Samkos Wildlife Sanctuary	3,334
	Seima Biodiversity Conservation Area	3,078
	Virachey National Park	3,339
Laos	Bokeo Nature Reserve	741
	Xe Pian – Dong Hoa Sao National Biodiversity Conservation Area	345
	Nakai Nam Theun National Protected Area	3,151
	Nam Et-Phou Louey National Protected Area	3,455
	Nam Kading National Protected Area	1,629
Vietnam	Bach Ma National Park	222
	Cat Tien National Park 1 (Nam Cat Tien sector)	465
	Cat Tien National Park 2 (Cat Loc sector)	338
	Song Thanh Nature Reserve	924
	Tam Dao National Park	342
	Van Ban Nature Reserve	380

In particular, there is a scarcity of imagery from the mid-1990s. For the sites in this study, a clear image was usually available from the late 1980s, but then frequently the next clear image available is not until the Landsat 7 era, starting in 1999. Thus, to try to make the periods over which change was measured approximately similar in length, three epoch dates of *c*.1990, *c*.2000 and *c*.2009 were chosen as target dates.

Imagery available in the USGS (US Geological Survey) Landsat archive for the seventeen path-row scenes required to cover the sites (Figure 20.1) was manually evaluated to identify suitable images for use in the analysis, using the following criteria:

- as close to epoch target dates (*c*.1990, *c*.2000 and *c*.2009) as possible, given other criteria;
- minimal cloud cover over the site;
- November to March date when possible, to minimize changes in vegetation due to annual phenological cycles (leaf on/leaf off, agriculture, etc.);
- similar or identical dates for sites that span the boundaries between different Landsat scenes (e.g. Nakai Nam Theun, Central Cardamoms), where possible. Note that it is often, but not always, possible to find same-date images for adjacent images in the same north–south path, as this is the orbital track. However, east–west adjacent images are never available on the same day;
- for recent images (2007–2009 time frame) where Landsat 7 is often the only choice, two images close in date to help fill the SLC gaps in each image.

The SLC gaps principally affect the east or west edges of the images, and do not affect the central third of the image, so they are a more significant issue for sites such as Nakai Nam Theun that are at the east or west edges of scene boundaries.

Given the available data and the above selection criteria, 61 images were selected for analysis (Table 20.2).

Methods

A major challenge in this study was to devise a methodology that would provide consistent results across the fifteen sites of the Lower Mekong region without the ability to conduct extensive independent ground-truthing. However, consultation with site managers at the final project workshop provided an opportunity for those familiar with each landscape to provide feedback on the analysis. This was taken into account during the preparation of this chapter. Analysing any one site can be relatively straightforward, and a variety of approaches may likely be successful, but would also rely upon the analyst making site and data-specific choices. To have consistent and comparable results across all sites, we developed a methodology that largely removed dependence on the analyst. The resulting methodology has four steps: (1) verification and correction of spatial fidelity; (2) imagery normalization; (3) change detection; (4) post-processing and results summary.

Spatial fidelity

All of the imagery used for this analysis is the USGS L1T product (Level 1 Terrain-corrected), which is an orthorectified dataset with sufficient spatial accuracy for images to overlay with less than 1 pixel error. However, we found that a few of the images showed noticeable spatial inaccuracies in some areas. These images were manually corrected by collecting tie points between the two images and shifting the incorrect image into place. In all cases, a simple shift was sufficient to correct the problem for the portion of the image of interest; imagery was not warped, or spatially stretched. After the initial analysis had been completed, many of the problematic images were reprocessed by USGS with improved geolocation. When possible, these reprocessed images were incorporated into the final analysis to minimize any errors due to spatial misregistration.

Imagery normalization

Our change detection methodology uses a vegetation index, MIRI (Mid Infra-Red Index), derived from near and mid infrared Landsat bands (more details on selection of this particular index in the change detection section below). To have an easily replicable methodology, this index needs to be comparable from

Table 20.2 Landsat imagery used for the analysis

Country	*Site*	*Estab.*	*Path/Row*	*Epoch 1*	*Epoch 2*	*Epoch 3a*	*Epoch 3b/4**
Cambodia	Central Cardamom PF and	2002	127/051	27-Mar-89 (4)	10-Jan-02 (7)	29-Jan-09 (7)	
	Phnom Samkos WS	1994	127/052	27-Mar-89 (4)	10-Jan-02 (7)	29-Jan-09 (7)	
	Mondulkiri PF	2002	124/051	30-Dec-90 (5)	03-Feb-01 (7)	10-Dec-09 (7)	26-Dec-09 (7)
			125/051	24-Jan-89 (4)	13-Feb-02 (7)	17-Mar-08 (7)	31-Jan-09 (7)
	Seima BCA	2002	125/051	24-Jan-89 (4)	13-Feb-02 (7)	17-Mar-08 (7)	31-Jan-09 (7)
			125/052	24-Jan-89 (4)	13-Feb-02 (7)	17-Mar-08 (7)	31-Jan-09 (7)
	Virachey NP	1993	125/050	24-Jan-89 (4)	27-Mar-00 (7)	29-Jan-08 (7)	17-Mar-08 (7)
Laos	Bokeo NR	1993?	130/046	11-Jan-89 (4)	24-Dec-99 (7)	16-Jan-08 (7)	18-Jan-09 (7)
	Xe Pian – Dong Hoa Sao NKNPA	2006	126/050	25-Dec-89 (5)	05-Dec-02 (7)	30-Jan- 09 (5)	
	Nakai Nam Theun NPA	1993	126/048	05-Apr-89 (4)	29-Sep-01 (7)	20-Jan-08 (7)	24-Dec-09 (7)
			127/047	11-Mar-89 (4)	04-Nov-00 (7)	10-Sep-09 (7)	
			127/048	11-Mar-89 (4)	04-Nov-00 (7)	10-Sep-09 (7)	
	Nam Et-Phou Louey NPA	1993	128/046	28-Dec-88 (4)	27-Dec-99 (7)	22-Dec-06 (5)	03-Dec-08 (7)*
	Nam Kading NBCA	1993	127/047	11-Mar-89 (4)	22-Dec-00 (7)	14-Feb-09 (7)	05-May-09 (7)
Vietnam	Bach Ma NP and Song Thanh NR	1937–86 2000	125/049	17-Feb-89 (5)	21-Apr-03 (7)	15-Mar-07 (7)	31-Mar-07 (7)
	Cat Tien NP 1 and 2	1978–98	124/052	30-Dec-90 (5)	05-Jan-02 (7)	22-Jan-08 (7)	07-Feb-08 (7)
	Tam Dao NP	1996	127/045	27-Dec-93 (5)	04-Nov-00 (7)	13-Jan-09 (7)	
	Van Ban NR	1997	128/045	01-Feb-93 (5)	27-Dec-99 (7)	04-Nov-06 (5)	03-Dec-08 (7)*

Notes: The Landsat satellite for each image (4, 5 or 7) is given in parentheses. For epoch 3, two images are used when available to help fill the data gaps resulting from the SLC failure on Landsat 7. In two cases – indicated by * – two images close in date were not available for epoch 3, so the change for a much shorter period (2006–2008) is computed, providing change for 3 periods: epoch 1–2, epoch 2–3, and epoch 3–4. The PA establishment date is also given; in cases indicated by a range of dates, initial protection is indicated by the first date, and current status by the second.

image to image, and site to site, and across ecoregions, such that similar index values represent similar vegetation conditions. The standard approach of first atmospherically correcting the Landsat bands did not consistently provide comparable MIRI indices for all images, likely due to insufficient ancillary atmospheric data, which are required for good correction. We were also unable to collect ground-truth data across all sites to provide a more empirical normalization. Instead, we developed a normalization approach based on image statistics.

In this approach we assume that the actual brightness of the brightest vegetation, as measured by the MIRI index, will be invariant across time and across the space of the image. That is, there will always be some pixels in any image, of a given area, with the brightest possible (for that area) MIRI values. Differences in that maximum value will thus be due to atmospheric or view differences, and not the intrinsic greenness of the vegetation. And we assume a similar logic for the darkest MIRI pixels. For some regions, such as deserts or savannahs, where the maximum vegetation signal may be very temporally dependent, these assumptions would not hold. However, as the region increases in size, it is more likely to contain pixels with maximum greenness. And, specifically, for the Lower Mekong region of this study and for the Landsat images, which are relatively large (approximately 185 km on a side, or 34,000 km^2), the assumption is valid; all clear Landsat images in this region will have some areas of dark green forests (= high MIRI values) and some areas with no vegetation (= low MIRI values).

We normalize the MIRI images by first locating sets of invariant dark (= non-vegetated) and bright (= dense vegetation) pixels in all images to be used for a given area. These invariant pixel sets are then used as end points for a linear normalization. The invariant sets are identified by thresholding the tails of the histogram of MIRI values for all input images; thus pixels that are, for example, *always* above 1 SD (standard deviation) from the mean for all image dates may be included in the bright target set. This set summarizes the consistently brightest vegetation across the set of images, and, as such, provides a useful and constant endpoint for normalization as we assume changes in this set are primarily determined by atmospheric or view effects, and do not indicate any fundamental difference in vegetation density on the ground. For some pixels, there may well be local changes in MIRI values, and so we require a relatively large set of pixels so that the set is representative of the image's maximum (or minimum) MIRI values. Since we are interested fundamentally in changes in vegetation, we choose these sets based on MIRI values, and not on other reflectance characteristics. Tests found that the resulting normalized images were not very sensitive to the specific number of pixels in the bright and dark sets, for a tested range from about 10,000 to 200,000 pixels (or 0.25–5 per cent of image pixels). In practice, the sets were determined by starting at 1.5 SD, and moving the threshold lower or higher, as needed, to get approximately 50,000–150,000 pixels in the final invariant set.

Once the dark and bright target sets were selected for the group of images, each image was normalized by stretching it linearly to the end points provided by the means from the image's set of dark and bright target pixels. This results in MIRI images showing little variance between dates for apparently unchanging areas. We confirmed these areas as unchanging by visually comparing to false-colour band combinations of the images.

Change detection

To identify forest degradation, we use a combination of two approaches: first, we use a change metric computed from multiple dates of imagery to identify pixels where vegetation has significantly changed between dates; and, second, we use a threshold on the earlier image's vegetation index to mask out changes in areas with non-forest vegetation.

The change metric chosen was the difference in vegetation density between the two imagery dates, as quantified by a mid-infrared reflectance index, MIRI. This is a simple variant on the traditional normalized difference vegetation index (NDVI; see Tucker 1979), and is computed from bands 4 (near-infrared) and 7 (mid-infrared) of Landsat imagery:

$$MIRI = \frac{(B4 - B7)}{(B4 + B7)}$$

MIRI was found more suitable than the more commonly used NDVI (derived similarly, but from red (Landsat band 3) and near infrared (band 4) reflectances), and another variant, IRI (Infra-Red Index) (derived using bands 4 and 5). Compared to NDVI, MIRI was found to generally have a higher value for areas of darker green vegetation (trees) than areas with brighter green vegetation, such as prime grasslands, which can have very high NDVI values. Compared to IRI, MIRI was found to be less sensitive to burn scars and other reflectance variations in exposed non-vegetated soil, which were a substantial concern in some sites.

The change metric is simply the difference in MIRI values for images at two dates:

$$VegChange_i > MIRI_{Date1} - MIRI_{Date2}$$

After computing *VegChange* for a pair of images, a threshold is applied to identify pixels where significant changes in vegetation have occurred. The threshold is determined empirically from the statistical distribution of *VegChange* values. We found that using a threshold of twice the standard deviation produced reasonable results; we evaluated the results visually, by comparing to false-colour composites of the imagery (typically, bands 5–4–3 in RGB). Thus, we are identifying pixels where *VegChange* is different than the mean *VegChange* value at a confidence level of 95 per cent:

Mark pixel *i* as Change if: $VegChange_i > \mu + 2\sigma$

where μ and σ are the mean and standard deviation of the image of *VegChange*, respectively.

Finally, we mask out areas of identified change that are not likely to represent closed forest (and thus high MIRI values) in the first image of the image pair. This helps remove change in lightly vegetated areas that may show significant changes in MIRI due to normal seasonal variations, or recent fire scars. To implement this, a threshold was manually selected from the first MIRI image of each pair by visually examining MIRI values across obvious forest–non-forest boundaries. In most cases, a threshold of 150 (where normalized MIRI images range from 0 to 200 in value) appeared suitable, but in some cases thresholds of 125 or 175 were selected, erring conservatively, to minimize change. Efforts were made to automate selection of this threshold, but a manual visual inspection was still found helpful to reconcile the results with what visual inspection of the imagery would suggest is likely occurring. This is discussed further below.

Post processing and results summary

After final change pixels are identified, a sieving operation is applied to clean up the results. Sieving is an operation in which any groups of contiguous pixels below a set size threshold are removed. It serves to remove possibly incorrect results that may result from slight mis-registration or other effects unrelated to the vegetation condition. For this analysis, a sieve threshold of 7 pixels was found helpful after evaluating several alternatives. For 30-metre pixels (= 0.09 hectares), this threshold leads to removal of isolated areas of change that are less than 0.63 hectare (7 × 0.09) in extent.

For sites that were split between different Landsat tiles, results are combined after the sieving operation.

Finally, the resulting change images are processed in a GIS (Geographic Information System) to sum the amount of change in each site and its surrounding buffer zone.

In a few cases, we have change indicated for a given pixel for both epochs (e.g. from both the *c*.1990–*c*.2000 and *c*.2000–*c*.2009 results). In such cases, the change was assigned only to the first image pair, on the assumption that the first change event was the most significant, such as from forest to secondary forest. Thus, subsequent change events, which may, for example, indicate further clearing of forest that was substantially thinned during the first epoch, are omitted from the tallied results. In all cases, the percentage of such pixels is small, and would not meaningfully affect the overall totals.

Results

Table 20.3 provides the tabulated forest degradation results for each site and buffer zone. In general, the results appear well supported by visual comparison

with the Landsat imagery. Partners in the region also confirmed the general validity of these results at the final project workshop, but no detailed ground-truthing has been completed. However, as the analysis was being conducted, certain limitations to the present methodology became clear (see the discussion section for more on this). Thus for PAs of particular interest, the raw imagery should be examined to determine if or where the results seem reasonable, given field data or local knowledge. A summary of observations on the results for each PA follows.

Cambodia

Central Cardamom Protected Forest and Phnom Samkos Wildlife Sanctuary

The analysis here generally appears well supported by visual inspection of the imagery. However, there are substantial areas with less dense vegetation that are harder to interpret, such as the central portion of Phnom Samkos where substantial 2002–2009 change is indicated. This area of change is sensitive to the minimum MIRI threshold. Field data would be useful for determining the best threshold or verifying the current results.

Mondulkiri Protected Forest and Seima Biodiversity Conservation Area

Mondulkiri appears to have very little dense forest cover. However, the change identified appears well supported by the imagery; overlapping areas from the neighbouring images provided similar results. Large areas of forest degradation appear just south of Seima. However, the degraded forest identified just west and south-west of Seima proper does not appear to have been dense forest; this change should be verified if of interest.

Virachey National Park

Little change appears to have occurred within the NP proper, but there is some definite forest degradation in nearby areas. The NP appears to contain both forested areas, and areas with more open woodlands, and the analysis had difficulty in separating the two landcover types with the MIRI threshold.

Laos

Bokeo Nature Reserve

The results for Bokeo show large areas of aggregated change in the buffer zone and scattered small areas within the PA itself. The change in the buffer zone is likely valid, but much of the change within the PA proper may related to phenological or topographic effects, and may not indicate a genuine degradation

Table 20.3 Forest degradation for all sites and surrounding 10-km wide buffer zones, provided as total area (km^2), % of area (core site or buffer zone), and % of area per year (% simply divided by length of epoch)

			Core protected area			*10 km buffer zone*		
	Protected area	*Epoch*	*km^2*	*%*	*%/year*	*km^2*	*%*	*%/year*
Cambodia	Central Cardamom PF	89–02	22.3	0.54	0.04	40.4	1.45	0.11
		02–09	11.7	0.32	0.05	27.8	1.21	0.17
	Phnom Samkos WS	89–02	20.5	0.62	0.05	45.3	2.12	0.17
		02–09	75.1	2.87	0.41	68.0	4.18	0.59
	Mondulkiri PF	89/90–01/02	6.8	0.17	0.01	4.6	0.15	0.01
		01/02–08/09	12.4	0.30	0.04	21.5	0.72	0.10
	Seima BCA	89–02	12.2	0.40	0.03	45.6	1.58	0.12
		02–08/09	33.6	1.09	0.16	200.1	6.94	1.00
	Virachey NP	89–00	3.0	0.09	0.01	26.1	0.70	0.06
		00–08	1.2	0.04	0.00	21.0	0.56	0.07
Laos	Bokeo NR	89–99	5.0	0.68	0.06	17.4	1.17	0.11
		99–08/09	10.4	1.41	0.16	45.5	3.05	0.34
	Dong Hoa Sao NBCA	89–02	4.2	1.21	0.09	6.1	0.61	0.05
		02–09	5.2	1.52	0.25	26.5	2.63	0.43
	Nakai Nam Theun NPA	89–00/01	32.0	1.12	0.10	10.7	0.49	0.04
		00/01–08/09	12.7	0.44	0.05	6.6	0.30	0.03

	Nam Et-Phou Louey NPA	88–99	17.5	0.51	0.05	35.7	0.86	0.08
		99–06	7.7	0.22	0.03	30.9	0.75	0.11
		06–08	3.8	0.13	0.07	13.4	0.38	0.20
	Nam Kading NPA	89–00	7.7	0.47	0.04	28.8	1.43	0.12
		00–09	12.9	0.79	0.10	149.0	7.43	0.91
Vietnam	Bach Ma NP	89–03	0.0	0.01	0.00	6.3	0.67	0.05
		03–07	4.4	1.99	0.51	22.7	2.42	0.62
	Song Thanh NR	89–03	5.4	0.59	0.04	35.6	1.73	0.12
		03–07	3.5	0.38	0.10	16.3	0.79	0.20
	Cat Tien NP 1 (Nam Cat)	90–02	0.1	0.02	0.00			
		02–08	2.8	0.60	0.10			
	Cat Tien NP 2 (Cat Loc)	90–02	0.9	0.27	0.02			
		02–08	6.4	1.91	0.32			
	Cat Tien Buffer	90–02				99.6	4.47	0.41
		02–08				93.2	4.30	0.71
	Tam Dao NP	93–00	0.1	0.02	0.00	1.2	0.09	0.01
		00–09	0.6	0.20	0.02	10.1	0.84	0.10
	Van Ban NR	93–99	1.5	0.39	0.06	9.3	0.73	0.11
		99–06	0.5	0.13	0.02	8.8	0.69	0.10
		06–08	1.3	0.36	0.17	4.9	0.41	0.20

of forest cover. Within the PA, there does not appear to be any area of large-scale permanent forest degradation. The high topographic relief and the deciduous phenology of Bokeo's dry monsoon forests complicate interpretation.

Xe Pian – Dong Hoa Sao National Biodiversity Conservation Area

The forest degradation here appears largely well supported by the imagery, and a large area of degradation is very clear just north-west of the PA. Note, however, that much of the PA (central portion) does not appear densely forested, so the results should be interpreted with field data. This may also explain why the degradation rate is higher within the PA than outside for the first epoch.

Nakai Nam Theun National Protected Area

This area is difficult to analyse because it lies at the intersection of three different Landsat scenes, and because optimal dates were not always available. In particular, for the *c*.2009 epoch, only a September image was available, and it is not clear if the vegetation condition at that time is strictly comparable to its condition at the dates of the other images (January and December). The analysis shows scattered change in the central portion of the PA that appears genuine, but similar areas are not always identified by the algorithm; there may be more change in this area than detected. In the north-western portion of the PA, the analysis shows degradation of forests along ridgelines in two areas. These areas are likely deciduous forests, which occur in this PA; intentional clearing would not have this pattern, and by *c*.2009, the forest appears to have recovered. The swampy (presumably) area in the buffer just south of the PA shows much change due to what appears to be local flooding in the *c*.2009 images. This is likely temporary, so results from this apparently flooded area are excluded from the results in Table 20.3. The higher recorded rate of degradation within the PA compared to the buffer also indicates that the results should be evaluated carefully.

Nam Et-Phou Louey National Protected Area

Much of the apparent change here appears temporary, and so may be related to phenological effects and not true forest degradation. As this PA is not primarily forested, but rather shrubland (as of 1997 *c*.63 per cent) (www.namet.org/about.html) or partially disturbed or open forest (23 per cent), the results from our methodology should be evaluated carefully.

Nam Kading National Protected Area

Little change is observed in the PA proper, but there is substantial degradation activity in the buffer zone.

Vietnam

Bach Ma National Park and Song Thanh Nature Reserve

These PAs appear to have suffered relatively little forest degradation, but the 10-km buffer zone shows substantially more activity. However, these images were difficult to analyse because of high haze (atmospheric humidity) in some of the images. The change analysis may be picking up change in vegetated but not forested areas; areas indicated as degraded should be carefully examined in concert with ground data to confirm the results.

Cat Tien National Park

The degradation observed here appears well supported, with very little change within the NP proper. However, clearly a large area of forest was lost just north of the Nam Cat Tien portion of the NP in the 1990–2002 period. The change in the north-west portion of the buffer may be in vegetation of lower density, and thus may not represent forest degradation.

Tam Dao National Park

The NP appears to have suffered very little forest degradation. The north-west slopes are heavily shadowed, and thus change analysis is not effective for those areas. Change identified outside the NP may or may not reflect changes in dense forested vegetation, as there does not visually appear to be substantial forest outside the NP proper. Thus, comparison of change rates between the NP and the surrounding buffer zone is of very limited utility.

Van Ban Nature Reserve

Small patches of change appear throughout both the PA and surrounding buffer, and appear well supported by visual examination. The larger areas of change along ridgelines to the north of the PA may originate from other effects on vegetation condition, such as deciduous leaf-drop, fire or drought conditions.

Figures 20.2 and 20.3 show a comparison of the detected degradation between the PAs considered in this study. Unsurprisingly, there is generally more degradation, both in absolute area terms and as a rate per area, in the surrounding buffer zones than in the PAs proper. In a few cases, this does not appear to be the case; Phnom Samkos shows a higher amount of degradation in the core than in the buffer for the *c*.2000–*c*.2009 epoch (Figure 20.2), but as a percentage of area, the core degradation is still lower (Figure 20.3). Note that the Vietnamese PAs appear fairly well protected, despite relatively large disturbances in the buffer zones immediately outside the sites. The Vietnamese PAs are also substantially smaller in total area (Table 20.1, average size of 445 km^2) than those in either Laos (average size 1,864 km^2) or Cambodia (3,594 km^2), and thus may be easier to protect.

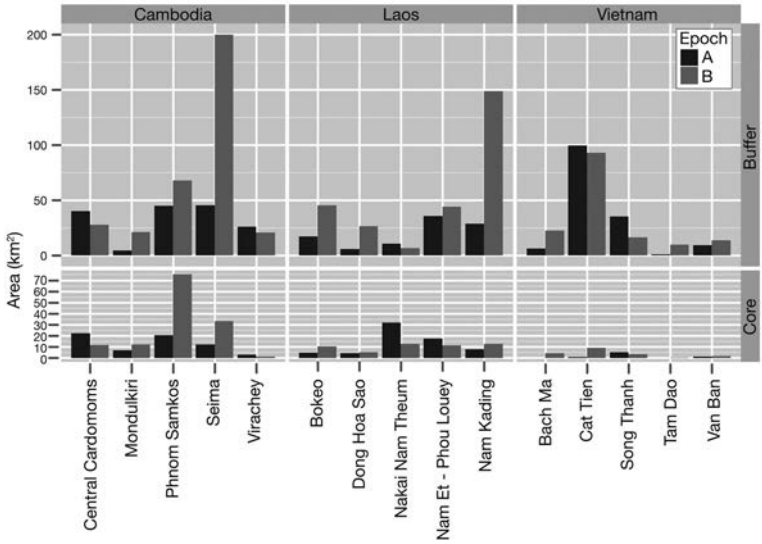

Figure 20.2 Forest degradation results, in area detected as degraded per epoch, per protected area

Source: Generated by Dan Slayback, NASA.

Notes: Area scale is constant between core and buffer. Epoch A = *c*.1990–*c*.2000, and epoch B = *c*.2000–*c*.2009. Cat Tien 1 and Cat Tien 2 PAs have been combined here to match against their combined buffer zone.

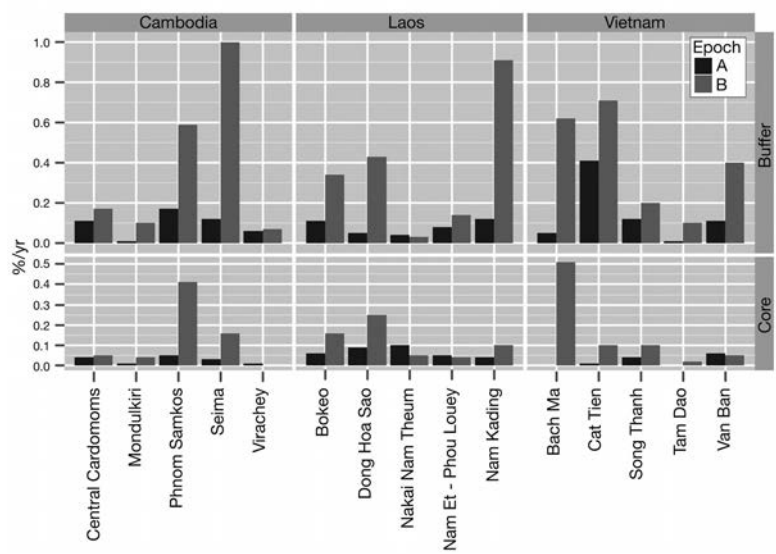

Figure 20.3 Forest degradation results, expressed as a percentage of the area degraded, per year

Source: Generated by Dan Slayback, NASA.

Notes: %/year scale is constant between core and buffer. Epoch A = *c*.1990–*c*.2000, and epoch B = *c*.2000–*c*.2009. Cat Tien 1 and Cat Tien 2 PAs have been combined here to match against their combined buffer zone.

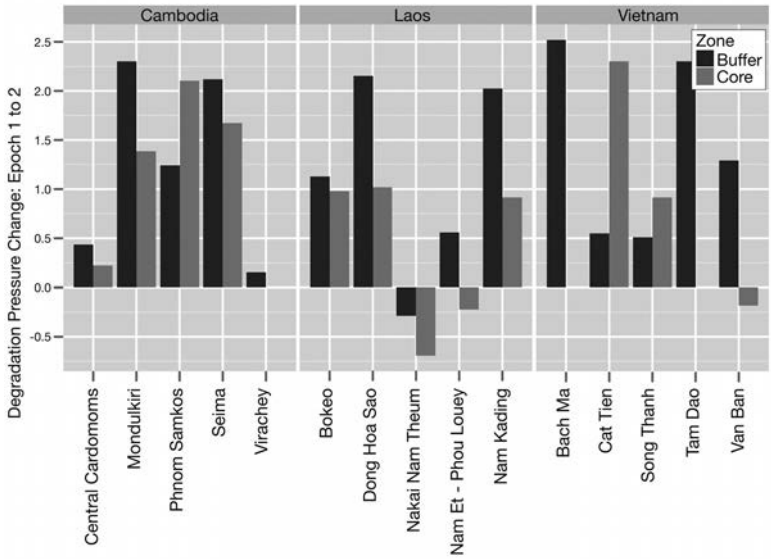

Figure 20.4 Change in degradation pressure from epoch A (*c*.1990–*c*.2000) to epoch B (*c*.2000–*c*.2009) for each site's core and buffer zones

Source: Generated by Dan Slayback, NASA.

Notes: "Pressure" is a relative term indicating the change in the yearly % degradation, and is here quantified as log(%ChangeEpochB/%ChangeEpochA). Thus values > 0 indicate increasing pressure, and < 0 indicate decreasing pressure. No value indicates that the epoch A change was so small that the ratio blows up (Virachey Core, Bach Ma Core, Tam Dao), and so a comparison of this type is not valid; we can simply say the pressure in those three cases is increasing.

In almost all cases, pressure on the forests appears to have increased between the *c*.1990–*c*.2000 and *c*.2000–*c*.2009 epochs, both within PAs proper and in buffer zones outside (Figure 20.4). This may reflect a real increase in degradation due to a real increase in pressure on forests.

Discussion

The change methodology appears to have been effective when good imagery is available, when the landcover appears to be forest dominated, and when we can reasonably assess the effectiveness of the method by visual examination of the raw imagery. The observed forest degradation suggests that forests are under increasing pressure, and also that many PAs have been fairly effective in limiting degradation within their borders; higher rates of degradation occur outside the PAs, except in two cases, one of which was problematic for several reasons (see Nakai Nam Theun comments above).

As the analysis was being conducted, certain limitations to the present methodology became clear. Thus, the numbers presented in Table 20.3 should be considered accordingly. For PAs of particular interest, the raw imagery should be examined to determine if or where the results seem reasonable, given field data or local knowledge, and additional field data collected if necessary.

Methodology limitations

The analysis methodology generally identifies change in vegetation density quite effectively. The primary limitation is determining where changes in vegetation density indicate changes in *forest* density as opposed to changes in vegetation density of other landcover, and where the changes are the effect of human activity versus either natural events or phenological cycles.

For this analysis, a threshold in the MIRI value of the first in the pair of images was applied to remove change in "non-forested" areas. More accurately, this removes change in less densely vegetated areas, which we assume are not forested. Although an automated procedure was preferred, and was one goal of the imagery normalization procedures, we found that adjusting the MIRI threshold manually, by visually interpreting the imagery and results, overall proved more reliable.

In some cases, changes due to human activity can be separated from those due to natural causes by spatial pattern. For example, in Nakai Nam Theun, we found apparent degradation along ridgelines that was unlikely to be caused by people, but rather perhaps by fire or as a natural consequence of deciduous leaf drop. However, for consistency, such areas have not been removed from the results presented.

The permanence of the identified forest degradation is another concern; areas identified as degraded in the *c*.1990–*c*.2000 period may, in some cases, then appear forested again in the *c*.2009 epoch. This may be due to genuine forest regrowth or recovery from the initial disturbance. But it may also indicate that the area is a secondary forest used in rotation with farming. Although our methodology can identify such regrowth areas, these were not specifically identified and quantified for this analysis. In all cases they were a very small fraction of the area identified as degraded.

Finally, the reported degradation rates per year should be interpreted cautiously. They are presented in an attempt to normalize observed changes over the different lengths of observation period and area. They can be used to compare rates between a core and buffer zone at a particular PA. However, comparing rates between epochs is more problematic, because differing lengths of time between the image pairs may capture change processes at different stages of regrowth or degradation. Note the nominal epochs (*c*.1990–*c*.2000 versus *c*.2000–*c*.2009) can differ by several years from the actual dates (Table 20.2).

Possible improvements

The present analysis was initiated under the assumption that there were significant areas of forests with relatively closed canopies, and that degradation of these forests was occurring due to clearing activities. However, these assumptions may not fully hold in all PAs; an improved analysis would take into account additional information about each PA's forested landcover. In particular, it would be useful to know the following:

1 The annual phenological cycle: are the forests deciduous, and if so, when are they leaf-off? What is the annual timing of herbaceous growth and senescence (for cases where herbaceous grasslands are an important landcover component). How much do these dates change from year to year?
2 What is the density of the forests that are of interest? Fully canopy closure, or open woodlands? Are they distinct from other landcover?
3 Do fires, droughts, or disease and insect outbreaks affect forest cover and phenology, and for how long before recovery?

With this information, and ground-truthing data from a sampling of locations, a standard classification procedure could be implemented on the sampled locations. Such analyses would then provide a useful validation of the current procedure, and possibly indicate areas for improvement.

Conclusion

The present analysis of forest degradation in fifteen protected areas in the Lower Mekong region of Cambodia, Laos, and Vietnam indicates that, by and large, the protected areas are not experiencing substantial forest degradation, although the surrounding areas may be. The analysis also shows the utility of remotely monitoring landcover trends, while some of the uncertainties of the analysis show the continued need for rigorously collected ground data.

References

Chape, S., Harrison, J., Spalding, M. and Lysenko, I. (2005) Measuring the extent and effectiveness of protected areas as an indicator of meeting global biodiversity targets, *Philosophical Transactions of the Royal Society (Botanical)* 360: 443–455.

Hardin, G. (1968) The tragedy of the commons. *Science* 162: 1243–1248.

Hutton, J.M., Adams, W.M. and Murombedzi, J.C. (2005) Back to the barriers? Changing narratives in biodiversity conservation. *Forum for Development Studies* 2: 341–370.

Porter-Bolland, L., Ellis, E., Guariguata, M., Ruiz-Mallen, I., Negrete-Yankelevich, S. and Reyes-Garcia, V. (2011) Community managed forests and forest protected area: an assessment of their conservation effectiveness in the tropics. *Forest Ecology and Management* doi:10.1016/j.foreco.2011.05.034.

Rayn, D. and Sutherland, W.J. (2011) Impact of nature reserve establishment on deforestation: a test. *Biodiversity and Conservation* 20: 1625–1633.

Robbins, P., McSweeney, K., Waite, T. and Rice, J. (2006) Even conservation rules are made to be broken: implications for biodiversity. *Environmental Management* 37(2): 162–169.

Rodrigues, A.S.L., Andelman, S.J., Bakarr, M.I., Boitani, L., Brooks, T.M., Cowling, R.M., Fishpool, L.D.C., da Fonseca, G.A.B., Gaston, K.J., Hoffmann, M., Long, J.S., Marquet, P.A., Pilgrim, J.D., Pressey, R.L., Schipper, J., Sechrest, W., Stuart, S., Underhill, L.G., Waller, R.W., Watts, M.E.J. and Yan, X. (2004) Effectiveness of the global protected area network in representing species diversity. *Nature* 428: 640–643.

Schmidt, C.B., Burgess, N.D., Coad, L., Belokurov, A., Besançon, C., Boisrobert, L., Campbell, A., Fish, L., Gliddon, D., Humphries, K., Kapos, V., Loucks, C., Lysenko, I., Miles, L., Mills, C., Minnemeyer, S., Pistorius, T., Ravilious, C., Steininger, M. and Winkel, G. (2009) Global analysis of the protection status of the world's forests. *Biological Conservation* 142: 2122–2130.

Tucker, C.J. (1979) Red and photographic infrared linear combinations for monitoring vegetation. *Remote Sensing of Environment* 8(2): 127–150.